High Pressure Electrochemical Reduction of CO_2 to Formic Acid/Formate: A Comparison between Bipolar Membranes and Cation Exchange Membranes

Mahinder Ramdin,[†] Andrew Morrison,[‡] Mariette de Groen,[¶] Rien van Haperen,[¶] Robert de Kler,[¶] Leo J. P. van den Broeke,[¶] J. P. Martin Trusler,[§] Wiebren de Jong,[‡] and Thijs J. H. Vlugt[*,†]

†*Engineering Thermodynamics, Process & Energy Department, Faculty of Mechanical, Maritime and Materials Engineering, Delft University of Technology, Leeghwaterstraat 39, 2628CB Delft, The Netherlands*

‡*Large-Scale Energy Storage, Process & Energy Department, Faculty of Mechanical, Maritime and Materials Engineering, Delft University of Technology, Leeghwaterstraat 39, 2628CB Delft, The Netherlands*

¶*Coval Energy, Wilhelminasingel 14, 4818AA Breda, The Netherlands*

§*Imperial College London, South Kensington Campus, London SW7 2AZ, United Kingdom*

E-mail: t.j.h.vlugt@tudelft.nl

Abstract

A high pressure semi-continuous batch electrolyzer is used to convert CO_2 to formic acid/formate on a tin-based cathode using bipolar membranes (BPMs) and cation exchange membranes (CEMs). The effects of CO_2 pressure up to 50 bar, electrolyte concentration, flow rate, cell potential, and the two types of membranes on the current density (CD) and Faraday efficiency (FE) for formic acid/formate are investigated. Increasing the CO_2 pressure yields a high FE up to 90% at a cell potential of 3.5 V and a CD of $\sim$30 mA/cm^2. The FE decreases significantly at higher cell potentials and current densities, and lower pressures. Up to 2 %wt formate was produced at a cell potential of 4 V, a CD of $\sim$100 mA/cm^2, and a FE of 65%. The advantages and disadvantages of using BPMs and CEMs in electrochemical cells for CO_2 conversion to formic acid/formate are discussed.

Introduction

The concept of producing chemicals and fuels from electricity, instead of fossil fuels, utilizing the intermittent behavior of renewable energy sources (i.e., power-to-X (P2X) concepts) has recently gained considerable interest from researchers aiming at reducing CO_2 emissions.[1–7] For example, CO_2 can be converted in an electrochemical cell to various value-added products like acids, alcohols, hydrocarbons, and syngas.[8–13] The selectivity of the different products depends on many process variables like the type of catalyst and its morphology, temperature, pressure, potential and current density, pH, electrolyte type and concentration, aqueous or non-aqueous solvent, flow characteristics, impurities, membranes, cell design, etc.[14–22] In aqueous solvents or solvents containing substantial amounts of water, the hydrogen evolution reaction (HER) is always in competition with the CO_2 reduction reaction (CRR).[23–25] This is because the solubility of CO_2 in water at standard conditions is low, which causes significant mass transfer limitations. To overcome this limitation, the use of non-aqueous solvents, gas-diffusion electrodes (GDEs), high CO_2 pressures, and cathodes which possess high over-

potentials for the HER, have been proposed.[14,26–31] However, the selectivity of an electrode for a certain product can change dramatically depending on the choice of the solvent. For example, the main product of CO_2 electrolysis on tin (Sn) or lead (Pb) electrodes in aqueous media is formic acid or formate, but this changes to oxalic acid/oxalate when a non-aqueous solvent is used.[32,33] Although GDEs have the potential to achieve high current densities, complex manufacturing techniques are required to assemble the different porous layers for optimal performance.[34–37] Despite all efforts in past years, it is still a challenge to find a stable catalyst and process conditions, which allow to obtain simultaneously a high Faraday efficiency (FE) and current density (CD) for a sufficiently long time. In practice this would mean that one has to compromise between CAPEX, which is dictated by the CD, and OPEX, which is mainly governed by the FE efficiency.[38–42] For a fixed product output, a low CD will require larger electrode surface areas, which will increase the size of the electrolyzer. A low FE will demand an increased input of resources (e.g., electricity, reactants, etc.) and additional downstream separation/recycling steps.

In this work, a high pressure semi-continuous batch electrolyzer is used to convert CO_2 to formic acid (HCOOH)/formate ($HCOO^-$), which is one of the simplest chemicals, requiring only two moles of electrons per mole of product, that can be obtained in an aqueous solvent. Formic acid (FA) is an interesting molecule, because it can be decomposed to hydrogen (decarboxylation) or carbon monoxide (decarbonylation).[43–46] FA is produced from CO_2 according to the following electrochemical half-cell reaction:

$$CO_2 + 2H^+ + 2e^- \longrightarrow HCOOH \tag{1}$$

The standard reduction potential of this reaction is -0.199 V vs. NHE at 298.15 K.[19] Note that this reaction does not imply a molecular mechanism, but it merely shows that two protons and electrons are required to obtain FA. Formic acid is a weak carboxylic acid with a pKa value of 3.74, which means that FA is only present in undissociated form at very

low pH values.[47] Therefore, CO_2 electroreduction at low pressures in alkaline solutions will mainly yield formate (i.e., the conjugate base of FA). However, as can be observed in Figure S1 of the Supporting Information, the pH of bicarbonate solutions drops significantly when high pressure CO_2 is dissolved. For this reason, whenever we refer to formic acid or formate in this paper, we essentially mean a mixture of both, whose distribution is governed by the pH. A tin-based electrode is used as the cathode, since it is known to exhibit a high Faraday efficiency (FE) towards formic acid production. Typically, an ion exchange membrane is used to prevent oxidation of the (liquid) products formed at the cathode, to avoid mixing of gaseous anodic (e.g., O_2) and cathodic (e.g., H_2) products, and to allow the use of different anolytes and catholytes (i.e., different pH conditions). Here, we investigate the effect of bipolar membranes (BPMs) and cation exchange membranes (CEMs) on the performance of the electrochemical reduction of CO_2. Anion exchange membranes (AEMs) were not tested in this study, because they exhibit a high formate crossover rate.[48] A CEM is a monopolar membrane with fixed negative charges, which allows cations to pass, but rejects anions.[49] A bipolar membrane is obtained by lamination of a positively charged anion exchange layer (AEL) and a negatively charged cation exchange layer (CEL), which are selective for anions and cations, respectively.[50,51] BPMs can be operated in two modes: (a) forward bias ($V > 0$), where the CEL of the membrane faces the anode, and (b) reverse bias ($V < 0$), where the CEL faces the cathode. In the forward bias mode, the electric field causes the mobile ions to migrate towards the interfacial region (IR), resulting in an accumulation of ions at the junction, which compensates the charges in the layers, thus decreasing the selectivity of the membrane.[52,53] As shown in Figure 1, in the reverse bias mode, applying a sufficiently high potential over the membrane will result in water splitting at the AEL-CEL interface due to; (1) chemical reactions of water with functional groups in the membrane, and (2) an enhanced electric field effect, which can be described by Onsager's theory of the second Wien effect.[50,54–60] The H^+ and OH^- ions will migrate through the CEL and AEL, respectively. In the reactor, the protons are then used in the CRR or HER, while the hydroxide ions are

discharged at the anode to produce water, oxygen, and electrons.

Bipolar membranes have several additional benefits over monopolar ion exchange membranes, like (1) BPMs allow the use of two different electrolyte solutions while maintaining a constant pH gradient over the membrane, (2) the product crossover is lower, and (3) acidification and basification can be performed without addition of acids and bases.[49,51,61] So far, BPMs have been applied in the electrodialysis process for acid and base production, CO_2 separation, water electrolysis, photo-electrolysis, fuel cells, water desalination, and, since recently, CO_2 electrolysis.[48,49,62–75] To the best of our knowledge, BPMs have not been used previously for high pressure CO_2 electrolysis to formic acid/formate.

In this work, for the first time, CO_2 electrolysis to formic acid/formate is performed at high pressures (up to 50 bars) using bipolar membranes. The experiments were also executed with cation exchange membranes to benchmark the performance of the BPMs. In addition, the effects of electrolyte flowrate, electrolyte concentration, CO_2 pressure, and cell potential on the Faraday efficiency of formate and current density are investigated. The advantages and disadvantages of using BPMs and CEMs for CO_2 electrolysis are discussed.

Experiments

An overview of the high pressure experimental setup is shown in Figure 2. The core of the setup is a high pressure electrochemical reactor, which can be operated up to 80 bar. In Figure 3, an exploded-view of the reactor is shown. The cell is divided into two compartments using either a bipolar ($\sim$160 μm, Fumasep FBM-PK, Fumatech) or a cation exchange ($\sim$130 μm, Fumasep FKB-PK, Fumatech) membrane. The cathodic compartment ($\sim$100 ml) is pressurized with high pressure CO_2 (99.999%, Linde Gas) from a gas cylinder and the catholyte is recirculated continuously with an HPLC-pump (Varian ProStar 210). The anodic compartment ($\sim$200 ml) can be pressurized either by a CO_2 or an N_2 gas cylinder, where the latter is used when supercritical CO_2 is required in the cathode compartment.

In this case, the CO_2 in the cathodic compartment is pressurized through the accumulator. The anodic and cathodic environment is separated by an accumulator, which prevents mixing of gases from both compartments and eliminates pressure differences over the membrane. The pressure difference over the membrane and the absolute pressure are measured with a differential pressure meter (Kobold, MAN-BF26-B4-A4-K) and a manometer (± 1 bar, Swagelok), respectively. A tin-based electrode (99.99%, ElectroCell) with a surface area of ∼140 cm^2 and an iridium mixed metal oxide (Ir-MMO, Magneto Special Anodes) mesh (∼180 cm^2) were used as the cathode and anode, respectively. We note, however, that the spacer covered a part of the cathode, which leads to a reactive surface area of the cathode of ∼80 cm^2. The volume of the anodic compartment and the surface area of the anode were larger than the volume of the cathodic compartment and the surface area of the cathode. The reason for this is that the anodic processes (e.g., oxygen evolution and water transport to the BPM) should not be the limiting factor for the cathodic CO_2 reduction reaction. The gap between the electrodes and the membrane was approximately 1 mm, which means that the electrode-to-electrode distance was ∼2 mm. The electrolytes potassium hydroxide (98% KOH), potassium bicarbonate (99.5% $KHCO_3$), and sulfuric acid (95% H_2SO_4) were purchased from Sigma-Aldrich and were used as received.

In a typical experiment, the reactor was loaded with approximately 200 ml of an anolyte and 100 ml of a catholyte, which was pressurized with high pressure CO_2 and recirculated for one hour with an HPLC-pump (∼10 ml/min) until saturation. Subsequently, electrolysis of CO_2 was performed for 20 minutes at a fixed cell potential using a lab power supply (Voltcraft DPPS-16-40). All experiments were performed at room temperature (22 ± 1 °C). During the experiments, the CO_2 in the buffer vessel was regularly flushed to prevent accumulation of gaseous reaction products, which might otherwise change the partial pressure of CO_2. At the end of each experiment, the anodic and cathodic compartments were completely emptied and the catholyte was analyzed for formic acid. The anolyte was only sampled randomly to determine the crossover of formic acid through the membranes. An Ion-Chromatograph

(Dionex DX-120, 4mm AG14/AS14 guard and analytical column) with suppressed conductivity detection was used to measure the formate concentration in the anolyte and catholyte. The flowrate of the eluent (1 mM Na_2CO_3/1 mM $NaHCO_3$ solution) was 1 ml/min. A pure standard of formic acid (Sigma-Aldrich) was used to calibrate the equipment for quantitative analysis.

It is well-known that tin-based electrodes can be affected by degradation/deactivation under cathodic polarization.[76] Therefore, after each experiment, the cathode was chemically treated with a 5% nitric acid (HNO_3) solution to remove possible deposits from the surface. Using a CEM with concentrated (> 0.5M) H_2SO_4 solutions as the anolyte resulted in some yellow sulfur-like deposition on the Ir-MMO anode surface, which was removed by reaction with a concentrated KOH solution. After treating the electrodes, both compartments were thoroughly rinsed with demineralized water and refilled with fresh electrolytes for the next experiment. The (bipolar) membranes were susceptible to abrupt pressure changes and startup/shutdown of the power supply. Therefore, the membranes were replaced after 15 pressurizing/depressurizing cycles. The reproducibility of the data was verified by repeating the experiments at least twice at the same operating conditions, but using fresh electrodes.

The Faraday efficiency and the current density are two important performance indicators in electrochemistry, just as selectivity and reaction rate are in traditional chemistry. The FE is a measure of how selectively electrons are transferred in an electrochemical reaction to the desired product. The FE (%) for formic acid/formate is calculated from:

$$\mathrm{FE} = \frac{FnVC^{\mathrm{exp}}}{ItM_w} \times 100\% \tag{2}$$

where I is the current (A = Coulombs/s), t is the total time of the experiments (s), M_w is the molecular weight of formic acid (g/mole), n the number of electrons involved in the reaction (2 for formic acid), V is the volume of catholyte (m^3), C^{exp} is the experimentally measured concentration of formic acid (g/m^3), and F the Faraday constant (Coulombs/mole). The

uncertainty in the FE can be evaluated from the individual uncertainties of the variables in Equation (2) using the methods of error propagation:[77]

$$\frac{\delta \mathrm{FE}}{\mathrm{FE}} = \sqrt{\left(\frac{\delta V}{V}\right)^2 + \left(\frac{\delta C}{C}\right)^2 + \left(\frac{\delta I}{I}\right)^2 + \left(\frac{\delta t}{t}\right)^2} \tag{3}$$

Using the estimated uncertainties of V ($\pm$ 1 ml due to purging), C ($\pm$ 1% due to the accuracy of the Ion-Chromatograph), I ($\pm$ 0.05 Amps due to the accuracy of reading), and t ($\pm$ 20 seconds due to manual start/shutdown of the power supply), the expected uncertainty in FE is ca. 5%.

The CD is calculated as the ratio between the current and the reactive geometrical surface area of the cathode ($\sim$80 cm^2). Since the current was not always constant during the experiments, the current versus time ($I - t$) curve was integrated to obtain the total charge passage (Q):

$$Q = \int_0^t I dt \tag{4}$$

The lab power supply allowed to read the current to an accuracy of 0.05 Amps, which imparts an uncertainty of 60 Coulombs on Q for a total measurement time of 20 minutes or an uncertainty in the CD of $\sim$0.6 mA/cm^2. The error due to the integration of Equation (4) is within this uncertainty.

Results and Discussion

In the following, the effect of CO_2 pressure, electrolyte concentration, catholyte flowrate, and cell potential on the CRR will be discussed. In addition, we show that the interplay between electrodes, electrolytes, and membranes is crucial for an efficient design of CO_2 electrolyzers. Finally, the advantages and disadvantages of BPMs and CEMs for CO_2 electrolysis are discussed.

Effect of CO_2 pressure

The aim of the first set of experiments was to investigate the effect of pressure on the electrochemical reduction of CO_2 to formate on a tin-based cathode using a BPM. In these experiments, the cell potential, temperature, pressures, flow rate, anolyte, and catholyte, were, 3.5 V, 22 ± 1 °C, 5 to 50 bar, 10 ml/min, 1M KOH, and 0.5M $KHCO_3$, respectively. The electrochemical experiments were performed as described in the experimental section and the results are shown in Figure 4. Clearly, the concentration of formate, the FE, and the CD sharply increase as the CO_2 pressure is increased, but the FE seems to reach a plateau (∼90 %) at around 40 bar. At these experimental conditions, increasing the pressure further does not improve the FE. In fact, a slight decrease in the FE is observed after a pressure of 40 bar, which is likely caused by (1) formate crossover through the BPM, and (2) a significant pH-drop caused by high pressure CO_2 dissolution, which favors the HER. Analysis of the anolyte confirmed that approximately 1% formate passed through the BPM.

The effect of pressure on the performance of CO_2 electrolysis to formate using cation exchange membranes was also investigated. The first experiments with a CEM were performed at 3.5 V, 22 ± 1 °C, pressures between 10 and 50 bars, 0.5M H_2SO_4 as the anolyte, 1M $KHCO_3$ as the catholyte, and a catholyte flow rate of 10 ml/min. In Figure 5, the results of the three different runs are shown. The conclusions for the CEM are very similar to the BPM; the FE, CD, and the concentration of formate increased as the CO_2 pressure is increased. The FE shows a maximum of ∼90 % around a CO_2 pressure of 40 bar with a slight decrease thereafter, which is again due to formate crossover through the CEM, and a pH-drop caused by CO_2 dissolution. Analysis of the anolyte confirmed that around 5% of the formate passed through the CEM, which is known to have a substantially higher product crossover than BPMs. Otherwise, a comparison of Figures 4 and 5 reveals that the performance of the CEM is very similar to the BPM. However, the CO_2 pressure seems to have a stronger influence on the FE of the CEM than for the BPM. A possible explanation for this is that as soon a potassium ion is pulled through the CEM, additional CO_2 becomes available via

bicarbonate decomposition:

$$HCO_3^- + H^+ \leftrightarrow CO_2 + H_2O \tag{5}$$

The equilibrium constant (K) of this reaction equals:

$$K = \frac{[CO_2]}{[HCO_3^-][H^+]} \tag{6}$$

Since the concentration of CO_2 in the solution is proportional to the pressure of CO_2, the equilibrium is shifted towards the right as the pressure is increased. The consequence of this is that more CO_2 becomes available locally in the solution, which promotes the CRR and increases the FE for formate formation.

The overall behavior observed for the BPM and the CEM can be explained as follows. At low pressures, the CO_2 solubility is low and the protons coming from the BPM/CEM mainly participate in the HER, instead of the CRR, thereby decreasing the FE for formate. At high pressures, the low solubility problem is (partially) resolved, but now the low current density or proton availability starts to limit the electrochemical process. To maximize the selectivity, it is important that CO_2, protons, and electrons are available in a correct stoichiometry at the electrode surface, which is qualitatively explained in Figure 6. Similar diagrams have been used by Hara et al.[26] and Li and Oloman[78,79] to explain product selectivities. Being a qualitative diagram, the size and boundaries of the regions in Figure 6 are chosen arbitrarily, but this will not interfere with the interpretation of the results. There is a small operating window, region 1 in Figure 6, where the supply of CO_2, electrons, and protons are correctly balanced. In principle, it is possible to have a high FE at low CDs, but for formic acid the highest FE is observed at moderate CDs and not a the lowest CD.[30] For this reason, region 1 is not extended to the right corner (region 3) of Figure 6. In all the other regions in Figure 6, there is either a defficiency in CO_2, protons, or electrons, which will adversely affect the selectivity. For example, region 2 is deficient in CO_2 and electrons, region 3 is

deficient in H^+ and electrons, region 4 is deficient in CO_2 and H^+, region 5 is deficient in electrons, region 6 is deficient in H^+, and region 7 is deficient in CO_2. A deficiency in CO_2, electrons, and protons corresponds to a state which is limited by mass transfer, kinetics, and water splitting, respectively. The key is to find the operating conditions that satisfy the requirements for region 1, which is a challenging task since in electrochemistry many of these parameters (i.e., potential, current density, concentration, FE) are non-linearly interrelated.

Effect of electrolyte concentration

The concentration of the catholyte can have a significant influence on the CO_2 electrolysis performance. Therefore, CO_2 electrolysis was performed at 3 V using a BPM, 1M KOH as the anolyte, a flow rate of 10 ml/min, and catholytes with three different (0.1M, 0.5M, and 1M) $KHCO_3$ concentrations. As shown in Figure 7, the highest FE and CD are obtained when an intermediate concentration of 0.5M $KHCO_3$ is used. Using a high concentration of $KHCO_3$ (1M) has a detrimental effect on the electrochemical reduction of CO_2, which is consistent with the literature and can be explained as: (1) the CO_2 solubility decreases significantly due to a salting-out effect, (2) an increased adsorption of potassium ions on the electrode inhibits CO_2 transport, (3) a buffering effect of HCO_3^- at the cathode, which decreases the surface pH as the bicarbonate concentration in the bulk is increased, and (4) the electric field is reduced, which destabilizes the CRR intermediates, thereby reducing the FE.[78–82] Using a low concentration of $KHCO_3$ (0.1M) suffers from a low conductivity and a significant pH-drop due to high pressure CO_2 dissolution. Both effects enhance the HER and reduce the FE for formate. Therefore, the performance of CO_2 electrolysis in terms of the FE and CD is better for moderate $KHCO_3$ concentrations: 0.5M > 0.1M > 1M.

The effect of electrolyte concentration on the CRR using a CEM was also investigated. CO_2 electrolysis was performed at 3.5 V, a flow rate of 10 ml/min, and three different combinations of anolyte (H_2SO_4) and catholyte ($KHCO_3$) concentrations, but keeping an anolyte to catholyte molar ratio of 1:2. The data in Figure 8 show that the combination

of 0.5M H_2SO_4 and 1M $KHCO_3$ gives the best results in terms of formate production, FE, and CD. The combination of 1M H_2SO_4 and 2M $KHCO_3$ is slightly better than the combination of 0.25M H_2SO_4 and 0.5M $KHCO_3$, especially in the higher pressure range. The optimal catholyte concentration for the CEM seems to be around 1M $KHCO_3$, while this was 0.5M $KHCO_3$ for the BPM. As explained earlier, in the case of the CEM, additional CO_2 is generated in the solution due to bicarbonate decomposition, which compensates for the salting-out effect of CO_2 at moderate $KHCO_3$ concentrations. However, the salting-out effect is dominant at very high $KHCO_3$ concentrations, which affects the CRR. At low electrolyte concentrations, the conductivity is lower, which increases the over-potential and mainly affects the current density.

The variability in the data of the BPM and the CEM is mainly caused by the condition of the membranes and the electrodes. After several experiments, scaling and/or fouling was observed for both the membrane types. Therefore, the membranes were replaced after 15 experiments (i.e., after three runs at five pressures). However, a new membrane (i.e., the first run) always gave a higher FE, CD, and formate concentration compared to the second and third runs. Furthermore, using a concentrated H_2SO_4 solution as the anolyte resulted in a yellow sulfur-like deposition on the Ir-MMO anode, which reduces the reactive surface area for the oxygen evolution reaction. This sulfur-like deposition was removed by reaction with a concentrated KOH solution. Similarly, a black deposit was observed on the Sn cathode, which was removed by reaction with a HNO_3 solution. Consistently applying these precautions results in a reproducibility of the experiments to within 5%. Due to the inherent variability in electrochemical experimental data, it is crucial to run multiple repeated experiments. The used tin electrodes were analyzed with a scanning electron microscope (SEM), see the Supporting Information for more details. The observed deposit on the electrode is very likely a tin oxide layer with some metal (e.g., copper) contamination. Agarwal et al.[38] observed similar deposits on Sn electrodes, which were characterized as graphitic type of carbon.

Effect of catholyte flowrate

It is well-known that stirring in batch reactors and flow characteristics in continuous flow reactors have a large impact on CO_2 electrolysis.[83–85] Therefore, the effect of catholyte flow rate on CO_2 electrolysis to formate at a cell potential of 3 V using a BPM was investigated. Two flow rates (10 ml/min and 20 ml/min) at several CO_2 pressures were tested using 1M KOH as the anolyte and 0.5M $KHCO_3$ as the catholyte. At low pressures, the experiments with a flow rate of 20 ml/min, compared to 10 ml/min, seems to perform slightly better in terms of FE and CD, see Figure 9. This is conform expectation, since increasing the flow rate decreases the thickness of the diffusion boundary layer, which improves mass transport of CO_2 to the electrodes. Often, mass transport is correlated with the Sherwood number, $\mathrm{Sh} = a\mathrm{Sc}^b\mathrm{Re}^c$, which is a function of the Schmidt (Sc) number and the Reynolds (Re) number. In laminar flows between two parallel plates, the exponents b and c are 1/3, thus the diffusion boundary layer thickness is proportional to $v^{-1/3}$, where v is the velocity of the fluid.[70,86] Therefore, it is surprising to see that at high pressures, the experiments with a flow rate of 10 ml/min have a higher FE and CD, which is opposed to the trend observed for low pressures. A possible explanation for this behavior is that mass transfer of CO_2 to the electrode is not the limiting factor at high pressures, since the solubility of CO_2 is relatively high, but other factors (like proton transport from the BPM to the electrode or increased impurity deposition on the cathode) come into play for increasing flow rates. This explanation is merely a hypothesis, which should be verified in the future with more detailed flow experiments and numerical modeling. Nevertheless, we note that Proietto et al.,[76] Alvarez-Guerra et al.,[87] and Li and Oloman[78,79,88] also observed that increasing the catholyte flow rate does not necessarily improve the performance of electrolytic CO_2 reduction.

Effect of cell potential

The cell potential can have a significant influence on the selectivity of products in an electrochemical cell. For this reason, CO_2 electrolysis was performed at three different cell potentials (i.e., 3 V, 3.5 V, and 4 V) using a BPM, 1M KOH as anolyte, 0.5M $KHCO_3$ as catholyte, 10 ml/min flow rate, 20 minutes electrolysis time, and pressures between 10 and 50 bar. The results for the three different cell potentials are depicted in Figure 10. For all three potentials, the concentration of formate, the FE, and the CD increase as the CO_2 pressure is increased. The FE seems to have a maximum around 40 bar for the 3 V and 3.5 V experiments, while this is absent at 4 V. However, the FE at 4 V (relative to 3 V and 3.5 V) is significantly lower in the low pressure range, which is due to an increased hydrogen production. At low pressures and low current densities, the system is initially located in region 2 of Figure 6. Since the CO_2 solubility and the CD increase at higher pressures, the systems shifts first towards region 5, and then (close) to region 1 of Figure 6. A FE of $\sim$90% is attainable at a cell potential of 3.5 V and a current density of $\sim$30 mA/cm^2, which results in a formate concentration of $\sim$1 %wt. At a cell potential of 4 V and low CO_2 pressures, the system is located in region 7 of Figure 6, and shifts very slowly towards region 1 for higher pressures. A FE of $\sim$65% is attainable at a cell potential of 4 V and a current density of $\sim$100 mA/cm^2, which results in a formate concentration of $\sim$2 %wt. At high current densities, the CO_2 is quickly consumed and mass transfer starts to limit the process, even at a pressure of 50 bar. Note that increasing the pressure further will have a minor effect, since the solubility of CO_2 in aqueous electrolyte solutions at temperatures below the critical point of CO_2 ($\sim$304 K) does not increase significantly at pressures close to or higher than the vapor pressure of CO_2. At these conditions, the CO_2-aqueous electrolyte system has a liquid-liquid behavior, which leads to low CO_2 solubilities. Increasing the temperature will improve the mass transfer of CO_2 and the electrode kinetics such that high current densities can be achieved at lower cell potentials, but the CO_2 solubility in aqueous solvents decreases significantly at higher temperatures. Alternatives to increase the CO_2 solubility are the use

of non-aqueous solvents, and electrolytes which exhibit a salting-in effect for CO_2. An ideal solvent should have a high CO_2 capacity, which is nearly independent of the temperature. In summary, at the given experimental conditions it is extremely challenging to obtain a high FE and a high CD at the same time. In practice, this would mean that one has to compromise between CAPEX, which is dictated by the current density, and OPEX, which is a function of the FE efficiency.

Combination of electrodes, electrolytes, and membranes

For a synergistic design of an electrochemical cell it is important that electrodes, electrolytes, and membranes are combined carefully. For example, an efficient operation of the BPM in the reverse bias mode requires an alkaline anolyte to decrease the overpotential for the oxygen evolution reaction (OER). However, it is not practical to use bicarbonate solutions as the anolyte, since the bicarbonate ions will react with the hydroxide ions from the BPM to form carbonates:

$$HCO_3^- + OH^- \leftrightarrow CO_3^{2-} + H_2O \tag{7}$$

The CRR is more efficient in neutral to (slighlty) alkaline solutions, but one should not use hydroxides (e.g., KOH) or carbonates (e.g., K_2CO_3) as the catholyte, because it will be converted to bicarbonates as the solution is saturated with CO_2:

$$KOH + CO_2 \leftrightarrow KHCO_3 \tag{8}$$

$$K_2CO_3 + CO_2 + H_2O \leftrightarrow 2KHCO_3 \tag{9}$$

Furthermore, using an alkaline solution as a catholyte (e.g., $KHCO_3$) in combination with a BPM will result in an additional voltage drop due to reactions of protons with bicarbonate ions at the catholyte-CEL interface. As can be seen in Figure 11, using an acidic anolyte (0.1M H_2SO_4) in combination with a BPM has a dramatic effect on the performance of the

electrochemical cell and the CRR. The current density and the amount of formate is reduced drastically compared to the data for an alkaline anolyte (i.e. 1M KOH). It is not efficient to use acidic anolytes in combination with BPMs, because the overpotential for the OER is higher in acidic media, and an additional potential drop is caused by acid-base reactions at the anolyte-AEL interface. In acidic media, water is split at the anode according to the reaction:

$$\mathrm{H_2O} \rightarrow 2\mathrm{H^+} + 2\mathrm{e^-} + \frac{1}{2}\mathrm{O_2} \tag{10}$$

The protons will react with the hydroxide ions from the BPM at the anolyte-AEL interface to cause an unnecessary potential drop, which can be estimated using a Nernst-like equation:

$$V_{\mathrm{loss}} \sim \frac{2.303RT}{nF} \log\left(\frac{[\mathrm{H^+}]^{\mathrm{anol.}}}{[\mathrm{H^+}]^{\mathrm{AEL}}}\right) \approx 0.059\Delta\mathrm{pH} \tag{11}$$

where R, T, n, F, $[\mathrm{H^+}]^i$ and ΔpH are the ideal gas constant, (room) temperature, charge of a proton, Faraday's constant, concentration of protons in the anolyte and AEL, and the pH difference between the anolyte and the AEL, respectively. Assuming that the concentration of hydroxide ions in the AEL is 1M (i.e., the pH is 14) and the pH of 0.1M H_2SO_4 is around 1, the potential drop is approximately 0.77 V. In contrast to BPMs, CEMs require acidic anolytes to function properly. Therefore, one should carefully select anolytes and catholytes for CO_2 electrolysis using BPMs/CEMs. In addition, it is important to select electrode materials/catalysts that have a high activity towards the desired oxidation/reduction reactions, and a high stability in acidic and alkaline environments. Recently, McCrory et al.[89] screened a large number of electrocatalysts for the HER/OER in acidic and alkaline solutions. Similar protocols should be used to screen electrocatalysts for the CRR in acidic, neutral, and alkaline environments.

Comparison between BPMs and CEMs for CO_2 electrolysis

The use of BPMs and CEMs for CO_2 electrolysis has a couple of advantages and disadvantages, see Table 1.[49,51,90–97] The main advantage of a BPM is that it can maintain a constant pH gradient over time when no acids or bases are formed as products.[53,70,71] This is not the case for CEMs, which continuously changes the pH balance of both compartments as cations are transported through the membrane. The consequence of this is that the anolyte is contaminated with cations from the catholyte and vice versa, which in the longer term will require purification of the electrolytes. Other advantages of BPMs include; low product crossover/losses, the possibility to acidify and basify without the addition of acids and bases, and less fouling when the membrane is operated in the reverse-bias mode.[48,49,51] The disadvantage of BPMs include; (1) a high price, which is a consequence of using complex manufacturing procedures to laminate the layers, (2) a low stability of the anion exchange layer, especially in strong alkaline solutions, (3) a limit on electrolyte/product concentration to prevent crossover and deterioration of water splitting efficiency due to transport limitations, and (4) a short lifetime due to delamination of the layers.[49,51,94] The latter is mainly caused by an abrupt startup/shutdown leading to accumulation of water on the interface, and due to bicarbonate crossover, which is converted in the interfacial region of the BPM to CO_2 according to the reaction:

$$HCO_3^- + H^+ \leftrightarrow H_2CO_3 \leftrightarrow CO_2 + H_2O \tag{12}$$

The CO_2 expands at the membrane interface as soon the reactor is depressurized, which leads to blistering and delamination of the layers.

The advantages of CEMs are; (1) a low price, which is related to the easy manufacturing procedure, (2) a low potential drop, due to the lower thickness of the membrane, and (3) high stability of the cation exchange layer, which increases the lifetime.[49,51,94] However, the disadvantages of CEMs are more severe compared to BPMs; (1) a high product crossover/loss, (2)

the acidic environment inhibits the OER and requires noble metals, and (3) contamination of the anolyte with cations from the catholyte and vice versa, which will require expensive electrolyte purification steps downstream of the process. Due to the crossover of ions and products, the pH of the anolyte and catholyte changes continuously, which can adversely affect the performance of CO_2 electrolysis. Note that the crossover of formate can be inhibited to some extent by selecting a proper CEM.

Current status of CO_2 electroreduction to formic acid/formate

In Table 2, a summary of recent studies on CO_2 electrolysis to formic acid/formate in continuous flow electrolyzers using Sn-based GDEs and plates is provided. Clearly, GDE-based CO_2 electroreduction yields a higher CD, FA concentration, and FA production rate. However, it is important to note the CD and FA production rate in all the studies were calculated based on the geometric surface area, which can be significantly different from the real electrochemical surface area.[98,99] The relatively high FA concentration reported by Del Castillo et al.[100] and Yang et al.[101] for the GDE-based processes is mainly a consequence of using small amounts (around 0.2 ml) of catholyte and low flowrate/surface area ratios. The concentration of formic acid decreased significantly as the flowrate was increased. Nevertheless, the single pass FA concentration of Yang et al. is to the best of our knowledge the highest reported so far in the literature. The key of the 3-compartment process of Dioxide Materials studied by Yang et al.[101] and Kaczur et al.[102] is an imidazolium-based anion exchange membrane (Sustainion™), which exhibits a high conductivity and stability for CO_2 electrolysis. Yang et al. also showed the importance of selecting CEMs to prevent formate crossover. Alvarez-Guerra et al.[87] used a low pressure continuous flow electrolyzer to convert CO_2 to formic acid/formate. These authors obtained a relatively high FE, but the concentration of FA was very low. Proietto et al.[76,103] used a high pressure (up to 30 bar) undivided filter-press cell with an Sn plate as cathode to convert CO_2 to formic acid. The data reported by Proietto et al. shows that the performance of the cell was stable up to 20 hours, but

deteriorated rapidly afterwards. The results reported in this work are (slightly) better than those of Proietto et al., although we have used a cathode with a larger surface area.

For a commercially viable process it is important that all the components of the cell (e.g., membranes, anodes and cathodes) are stable for a sufficiently long-term. To the best of our knowledge, only the Sustainion-based CO_2 electroreduction process of Dioxide Materials has demonstrated stable operation for more than 500 hours for formic acid and up to 4000 hours for CO without showing significant loss of activity.[101,102] In this work, we have focused on the reproducibility of the results and long-term stability tests will be performed in a follow-up study.

Conclusions

The electrochemical reduction of CO_2 to value-added products will play an important role in power-to-X (P2X) concepts where renewable energy sources, instead of hydrocarbons, are used to produce chemicals and fuels. Before CO_2 utilization by the electrochemical route can be applied at a practical scale, a number of challenges need to be overcome. These include the poor stability and selectivity of the catalyst, the low solubility of CO_2, the separation of dilute products from electrolyte solutions, and the large overpotentials required to perform the reactions increase the power input/cost of the products. Here, we have used a high pressure semi-continuous batch electrolyzer to efficiently convert CO_2 to formic acid/formate. The effects of CO_2 pressure, cell potential, electrolyte concentration, flow rate, and two types of membranes, a bipolar membrane (BPM) and a cation exchange membrane (CEM), on the current density (CD) and Faraday efficiency (FE) for formate were investigated. The FE and the CD increase sharply with increasing CO_2 pressure. The results show that a FE of $\sim$90 % is attainable at a pressure of 40-50 bars, a cell potential of 3.5 V and a CD of $\sim$30 mA/cm^2. Up to 2 %wt formate was produced at a cell potential of 4 V, a CD of $\sim$100 mA/cm^2, but at a significantly lower FE of 65%. The results also indicate that a moderate flow rate and

catholyte ($KHCO_3$) concentration should be used to maximize the FE and CD. Although the operating principles of a BPM and a CEM are fundamentally different, they showed a similar performance for CO_2 electrolysis in terms of the FE and the CD. Nevertheless, BPMs and CEMs have some inherent advantages and disadvantages, which have been discussed in detail. In contrast to CEMs, BPMs can maintain a constant pH gradient over the membrane and have a low liquid product crossover, which is crucial for the economics of a large scale CO_2 electrolysis process. We have demonstrated that increasing the pressure has a beneficial effect on the performance of electrolytic CO_2 reduction to formic acid/formate.

Acknowledgement

The authors thank Michel van den Brink for his help with the Ion-Chromatograph. The project (TEEI116076: Direct electrochemical conversion of CO_2 to formic acid (P2FA)) is being carried out with subsidy from the Dutch Ministry of Economic Affairs, under the scheme Joint Industry Projects, executed by RVO (Rijksdienst voor Ondernemend Nederland). TJHV acknowledges NWO-CW (Chemical Sciences) for a VICI grant.

Supporting Information Available

A plot of pH as a function of CO_2 pressure in aqueous sodium bicarbonate solutions. SEM images and EDX spectra of the used tin electrodes.

References

(1) Gattrell, M.; Gupta, N.; Co, A. Electrochemical Reduction of CO_2 to Hydrocarbons to Store Renewable Electrical Energy and Upgrade Biogas. *Energy Convers. Manag.* **2007**, *48*, 1255–1265.

(2) Seh, Z. W.; Kibsgaard, J.; Dickens, C. F.; Chorkendorff, I.; Nørskov, J. K.; Jaramillo, T. F. Combining Theory and Experiment in Electrocatalysis: Insights into Materials Design. *Science* **2017**, *355*, eaad4998.

(3) Foit, S. R.; Vinke, I. C.; de Haart, L. G. J.; Eichel, R.-A. Power-to-Syngas: An Enabling Technology for the Transition of the Energy System? *Angew. Chemie Int. Ed.* **2017**, *56*, 5402–5411.

(4) Institute for Sustainable Process Technology, Power to Ammonia. *Report* **2017**, 51.

(5) Schemme, S.; Samsun, R. C.; Peters, R.; Stolten, D. Power-to-fuel as a Key to Sustainable Transport Systems - An Analysis of Diesel Fuels Produced from CO_2 and Renewable Electricity. *Fuel* **2017**, *205*, 198–221.

(6) Sternberg, A.; Bardow, A. Power-to-What? - Environmental Assessment of Energy Storage Systems. *Energy Environ. Sci.* **2015**, *8*, 389–400.

(7) Bernard, K.; Hernando, A. *Global outlook on energy technology development DTU International Energy Report 2018*; 2018.

(8) Azuma, M.; Watanabe, M. Electrodes in Low-Temperature Aqueous $KHCO_3$ Media. *J. Electrochem. Soc.* **1990**, *137*, 1772–1778.

(9) Bushuyev, O. S.; De Luna, P.; Dinh, C. T.; Tao, L.; Saur, G.; van de Lagemaat, J.; Kelley, S. O.; Sargent, E. H. What Should We Make with CO_2 and How Can We Make It? *Joule* **2018**, *2*, 825–832.

(10) Gattrell, M.; Gupta, N.; Co, A. A Review of the Aqueous Electrochemical Reduction of CO_2 to Hydrocarbons at Copper. *J. Electroanal. Chem.* **2006**, *594*, 1–19.

(11) Kuhl, K. P.; Cave, E. R.; Abram, D. N.; Jaramillo, T. F. New Insights into the Electrochemical Reduction of Carbon Dioxide on Metallic Copper Surfaces. *Energy Environ. Sci.* **2012**, *5*, 7050.

(12) Sheng, W.; Kattel, S.; Yao, S.; Yan, B.; Liang, Z.; Hawxhurst, C. J.; Wu, Q.; Chen, J. G. Electrochemical Reduction of CO_2 to Synthesis Gas with Controlled CO/H_2 Ratios. *Energy Environ. Sci.* **2017**, *10*, 1180–1185.

(13) Dinh, C.-T.; Burdyny, T.; Kibria, M. G.; Seifitokaldani, A.; Gabardo, C. M.; García de Arquer, F. P.; Kiani, A.; Edwards, J. P.; De Luna, P.; Bushuyev, O. S.; Zou, C.; Quintero-Bermudez, R.; Pang, Y.; Sinton, D.; Sargent, E. H. CO_2 Electroreduction to Ethylene via Hydroxide-mediated Copper Catalysis at an Abrupt Interface. *Science* **2018**, *360*, 783–787.

(14) Hori, Y. In *Solar to Chemical Energy Conversion*; Sugiyama, M., Fujii, K., Nakamura, S., Eds.; Lecture Notes in Energy; Springer International Publishing: Cham, 2016; Vol. 32; pp 191–211.

(15) Whipple, D. T.; Kenis, P. J. A. Prospects of CO_2 Utilization via Direct Heterogeneous Electrochemical Reduction. *J. Phys. Chem. Lett.* **2010**, *1*, 3451–3458.

(16) Lu, X.; Leung, D. Y. C.; Wang, H.; Leung, M. K. H.; Xuan, J. Electrochemical Reduction of Carbon Dioxide to Formic Acid. *ChemElectroChem* **2014**, *1*, 836–849.

(17) Kortlever, R.; Shen, J.; Schouten, K. J. P.; Calle-Vallejo, F.; Koper, M. T. M. Catalysts and Reaction Pathways for the Electrochemical Reduction of Carbon Dioxide. *J. Phys. Chem. Lett.* **2015**, *6*, 4073–4082.

(18) Feaster, J. T.; Shi, C.; Cave, E. R.; Hatsukade, T.; Abram, D. N.; Kuhl, K. P.; Hahn, C.; Nørskov, J. K.; Jaramillo, T. F. Understanding Selectivity for the Electrochemical Reduction of Carbon Dioxide to Formic Acid and Carbon Monoxide on Metal Electrodes. *ACS Catal.* **2017**, *7*, 4822–4827.

(19) Chaplin, R. P.; Wragg, A. A. Effects of Process Conditions and Electrode Material on Reaction Pathways for Carbon Dioxide Electroreduction with Particular Reference to Formate Formation. *J. Appl. Electrochem.* **2003**, *33*, 1107–1123.

(20) Jhong, H.-R. M.; Ma, S.; Kenis, P. J. Electrochemical Conversion of CO_2 to Useful Chemicals: Current Status, Remaining Challenges, and Future Opportunities. *Curr. Opin. Chem. Eng.* **2013**, *2*, 191–199.

(21) Zheng, X. et al. Sulfur-Modulated Tin Sites Enable Highly Selective Electrochemical Reduction of CO_2 to Formate. *Joule* **2017**, *1*, 794–805.

(22) Irabien, A.; Alvarez-Guerra, M.; Albo, J.; Dominguez-Ramos, A. *Electrochem. Water Wastewater Treat.*; Elsevier, 2018; pp 29–59.

(23) Liu, X.; Xiao, J.; Peng, H.; Hong, X.; Chan, K.; Nørskov, J. K. Understanding Trends in Electrochemical Carbon Dioxide Reduction Rates. *Nat. Commun.* **2017**, *8*, 15438.

(24) Ooka, H.; Figueiredo, M. C.; Koper, M. T. M. Competition between Hydrogen Evolution and Carbon Dioxide Reduction on Copper Electrodes in Mildly Acidic Media. *Langmuir* **2017**, *33*, 9307–9313.

(25) Zhang, Y.-J.; Sethuraman, V.; Michalsky, R.; Peterson, A. A. Competition between CO_2 Reduction and H_2 Evolution on Transition-Metal Electrocatalysts. *ACS Catal.* **2014**, *4*, 3742–3748.

(26) Hara, K. Electrochemical Reduction of CO_2 on a Cu Electrode under High Pressure. *J. Electrochem. Soc.* **1994**, *141*, 2097.

(27) Hara, K.; Kudo, A.; Sakata, T. Electrochemical Reduction of Carbon Dioxide Under High Pressure on Various Electrodes in an Aqueous Electrolyte. *J. Electroanal. Chem.* **1995**, *391*, 141–147.

(28) Hara, K.; Sakata, T. Large Current Density CO_2 Reduction under High Pressure Using Gas Diffusion Electrodes. 1997.

(29) Kaneco, S.; Iiba, K.; Katsumata, H.; Suzuki, T.; Ohta, K. Electrochemical Reduction of High Pressure CO_2 at a Cu Electrode in Cold Methanol. *Electrochim. Acta* **2006**, *51*, 4880–4885.

(30) Todoroki, M.; Hara, K.; Kudo, A.; Sakata, T. Electrochemical Reduction of High Pressure CO_2 at Pb, Hg and In Electrodes in an Aqueous $KHCO_3$ Solution. *J. Electroanal. Chem.* **1995**, *394*, 199–203.

(31) Mahmood, M. N.; Masheder, D.; Harty, C. J. Use of Gas-diffusion Electrodes for High-rate Electrochemical Reduction of Carbon Dioxide. I. Reduction at Lead, Indium- and Tin-impregnated Electrodes. *J. Appl. Electrochem.* **1987**, *17*, 1159–1170.

(32) Kai, T.; Zhou, M.; Duan, Z.; Henkelman, G. A.; Bard, A. J. Detection of CO_2^{*-} in the Electrochemical Reduction of Carbon Dioxide in N , N -Dimethylformamide by Scanning Electrochemical Microscopy. *J. Am. Chem. Soc.* **2017**, *139*, 18552–18557.

(33) Costentin, C.; Robert, M.; Savéant, J.-M. Catalysis of the Electrochemical Reduction of Carbon Dioxide. *Chem. Soc. Rev.* **2013**, *42*, 2423–2436.

(34) Bidault, F.; Brett, D.; Middleton, P.; Brandon, N. Review of Gas Diffusion Cathodes for Alkaline Fuel Cells. *J. Power Sources* **2009**, *187*, 39–48.

(35) Cindrella, L.; Kannan, A.; Lin, J.; Saminathan, K.; Ho, Y.; Lin, C.; Wertz, J. Gas Diffusion Layer for Proton Exchange Membrane Fuel Cells - A Review. *J. Power Sources* **2009**, *194*, 146–160.

(36) Park, S.; Lee, J.-W.; Popov, B. N. A Review of Gas Diffusion Layer in PEM Fuel Cells: Materials and Designs. *Int. J. Hydrogen Energy* **2012**, *37*, 5850–5865.

(37) Weng, L.-C.; Bell, A. T.; Weber, A. Z. Modeling Gas-diffusion Electrodes for CO_2 Reduction. *Phys. Chem. Chem. Phys.* **2018**, *20*, 16973–16984.

(38) Agarwal, A. S.; Zhai, Y.; Hill, D.; Sridhar, N. The Electrochemical Reduction of Carbon Dioxide to Formate/Formic Acid: Engineering and Economic Feasibility. *ChemSusChem* **2011**, *4*, 1301–1310.

(39) Jouny, M.; Luc, W.; Jiao, F. General Techno-Economic Analysis of CO_2 Electrolysis Systems. *Ind. Eng. Chem. Res.* **2018**, *57*, 2165–2177.

(40) Pérez-Fortes, M.; Schöneberger, J. C.; Boulamanti, A.; Harrison, G.; Tzimas, E. Formic Acid Synthesis Using CO_2 as Raw Material: Techno-economic and Environmental Evaluation and Market Potential. *Int. J. Hydrogen Energy* **2016**, *41*, 16444–16462.

(41) Spurgeon, J. M.; Kumar, B. A Comparative Technoeconomic Analysis of Pathways for Commercial Electrochemical CO_2 Reduction to Liquid Products. *Energy Environ. Sci.* **2018**, *11*, 1536–1551.

(42) Verma, S.; Kim, B.; Jhong, H.-R. M.; Ma, S.; Kenis, P. J. A. A Gross-Margin Model for Defining Technoeconomic Benchmarks in the Electroreduction of CO_2. *ChemSusChem* **2016**, *9*, 1972–1979.

(43) Moret, S.; Dyson, P. J.; Laurenczy, G. Direct Synthesis of Formic Acid from Carbon Dioxide by Hydrogenation in Acidic Media. *Nat. Commun.* **2014**, *5*, 1–7.

(44) Rahbari, A.; Ramdin, M.; van den Broeke, L. J. P.; Vlugt, T. J. H. Combined Steam Reforming of Methane and Formic Acid To Produce Syngas with an Adjustable H_2:CO Ratio. *Ind. Eng. Chem. Res.* **2018**, *57*, 10663–10674.

(45) Leitner, W. Carbon Dioxide as a Raw Material: The Synthesis of Formic Acid and Its Derivatives from CO_2. *Angew. Chemie Int. Ed. English* **1995**, *34*, 2207–2221.

(46) Rumayor, M.; Dominguez-Ramos, A.; Irabien, A. Formic Acid Manufacture: Carbon Dioxide Utilization Alternatives. *Appl. Sci.* **2018**, *8*, 914.

(47) Hietala, J.; Vuori, A.; Johnsson, P.; Pollari, I.; Reutemann, W.; Kieczka, H. *Ullmann's Encycl. Ind. Chem.*; Wiley-VCH Verlag GmbH & Co. KGaA: Weinheim, Germany, 2016; pp 1–22.

(48) Li, Y. C.; Yan, Z.; Hitt, J.; Wycisk, R.; Pintauro, P. N.; Mallouk, T. E. Bipolar Membranes Inhibit Product Crossover in CO_2 Electrolysis Cells. *Adv. Sustain. Syst.* **2018**, *2*, 1700187.

(49) Strathmann, H.; Grabowski, A.; Eigenberger, G. Ion-Exchange Membranes in the Chemical Process Industry. *Ind. Eng. Chem. Res.* **2013**, *52*, 10364–10379.

(50) Strathmann, H.; Krol, J. J.; Rapp, H.-J.; Eigenberger, G. Limiting Current Density and Water Dissociation in Bipolar Membranes. *J. Memb. Sci.* **1997**, *125*, 123–142.

(51) Tongwen, X. Electrodialysis Processes with Bipolar Membranes (EDBM) in Environmental Protection-A Review. *Resour. Conserv. Recycl.* **2002**, *37*, 1–22.

(52) Vargas-Barbosa, N. M.; Geise, G. M.; Hickner, M. A.; Mallouk, T. E. Assessing the Utility of Bipolar Membranes for use in Photoelectrochemical Water-Splitting Cells. *ChemSusChem* **2014**, *7*, 3017–3020.

(53) Vermaas, D. A.; Sassenburg, M.; Smith, W. A. Photo-assisted Water Splitting with Bipolar Membrane Induced pH Gradients for Practical Solar Fuel Devices. *J. Mater. Chem. A* **2015**, *3*, 19556–19562.

(54) Mafé, S.; Ramírez, P. Electrochemical Characterization of Polymer Ion-exchange Bipolar Membranes. *Acta Polym.* **1997**, *48*, 234–250.

(55) Mafé, S.; Manzanares, J. A.; Ramrez, P. Model for Ion Transport in Bipolar Membranes. *Phys. Rev. A* **1990**, *42*, 6245–6248.

(56) Ramírez, P.; Aguilella, V.; Manzanares, J.; Mafé, S. Effects of Temperature and Ion Transport on Water Splitting in Bipolar Membranes. *J. Memb. Sci.* **1992**, *73*, 191–201.

(57) Simons, R. Preparation of a High Performance Bipolar Membrane. *J. Memb. Sci.* **1993**, *78*, 13–23.

(58) Simons, R.; Khanarian, G. Water Dissociation in Bipolar Membranes: Experiments and Theory. *J. Membr. Biol.* **1978**, *38*, 11–30.

(59) Simons, R. A Mechanism for Water Flow in Bipolar Membranes. *J. Memb. Sci.* **1993**, *82*, 65–73.

(60) Simons, R. A Novel Method for Preparing Bipolar Membranes. *Electrochim. Acta* **1986**, *31*, 1175–1177.

(61) Huang, C.; Xu, T. Electrodialysis with Bipolar Membranes for Sustainable Development. *Environ. Sci. Technol.* **2006**, *40*, 5233–5243.

(62) Eisaman, M. D.; Alvarado, L.; Larner, D.; Wang, P.; Littau, K. A. CO_2 Desorption Using High-Pressure Bipolar Membrane Electrodialysis. *Energy Environ. Sci.* **2011**, *4*, 4031.

(63) Eisaman, M. D.; Alvarado, L.; Larner, D.; Wang, P.; Garg, B.; Littau, K. A. CO_2 Separation Using Bipolar Membrane Electrodialysis. *Energy Environ. Sci.* **2011**, *4*, 1319–1328.

(64) Grew, K. N.; McClure, J. P.; Chu, D.; Kohl, P. A.; Ahlfield, J. M. Understanding Transport at the Acid-Alkaline Interface of Bipolar Membranes. *J. Electrochem. Soc.* **2016**, *163*, F1572–F1587.

(65) Li, Y. C.; Zhou, D.; Yan, Z.; Gonçalves, R. H.; Salvatore, D. A.; Berlinguette, C. P.; Mallouk, T. E. Electrolysis of CO_2 to Syngas in Bipolar Membrane-Based Electrochemical Cells. *ACS Energy Lett.* **2016**, *1*, 1149–1153.

(66) McDonald, M. B.; Ardo, S.; Lewis, N. S.; Freund, M. S. Use of Bipolar Membranes for Maintaining Steady-State pH Gradients in Membrane-Supported, Solar-Driven Water Splitting. *ChemSusChem* **2014**, *7*, 3021–3027.

(67) Luo, J.; Vermaas, D. A.; Bi, D.; Hagfeldt, A.; Smith, W. A.; Grätzel, M. Bipolar Membrane-Assisted Solar Water Splitting in Optimal pH. *Adv. Energy Mater.* **2016**, *6*, 1600100.

(68) Reiter, R. S.; White, W.; Ardo, S. Communication-Electrochemical Characterization of Commercial Bipolar Membranes under Electrolyte Conditions Relevant to Solar Fuels Technologies. *J. Electrochem. Soc.* **2016**, *163*, H3132–H3134.

(69) Salvatore, D. A.; Weekes, D. M.; He, J.; Dettelbach, K. E.; Li, Y. C.; Mallouk, T. E.; Berlinguette, C. P. Electrolysis of Gaseous CO_2 to CO in a Flow Cell with a Bipolar Membrane. *ACS Energy Lett.* **2018**, *3*, 149–154.

(70) Vermaas, D. A.; Wiegman, S.; Nagaki, T.; Smith, W. A. Ion Transport Mechanisms in Bipolar Membranes for (Photo)electrochemical Water Splitting. *Sustain. Energy Fuels* **2018**, *2*, 2006–2015.

(71) Vermaas, D. A.; Smith, W. A. Synergistic Electrochemical CO_2 Reduction and Water Oxidation with a Bipolar Membrane. *ACS Energy Lett.* **2016**, *1*, 1143–1148.

(72) Zhou, X.; Liu, R.; Sun, K.; Chen, Y.; Verlage, E.; Francis, S. A.; Lewis, N. S.; Xiang, C. Solar-Driven Reduction of 1 atm of CO_2 to Formate at 10% Energy-Conversion Efficiency by Use of a TiO_2-Protected III-V Tandem Photoanode in Conjunction with a Bipolar Membrane and a Pd/C Cathode. *ACS Energy Lett.* **2016**, *1*, 764–770.

(73) Mani, K. Electrodialysis Water Splitting Technology. *J. Memb. Sci.* **1991**, *58*, 117–138.

(74) Jaime-Ferrer, J. S.; Couallier, E.; Viers, P.; Durand, G.; Rakib, M. Three-Compartment Bipolar Membrane Electrodialysis for Splitting of Sodium Formate into Formic Acid and Sodium Hydroxide: Role of Diffusion of Molecular Acid. *J. Memb. Sci.* **2008**, *325*, 528–536.

(75) Jaime-Ferrer, J.; Couallier, E.; Viers, P.; Rakib, M. Two-Compartment Bipolar Membrane Electrodialysis for Splitting of Sodium Formate into Formic Acid and Sodium Hydroxide: Modelling. *J. Memb. Sci.* **2009**, *328*, 75–80.

(76) Proietto, F.; Schiavo, B.; Galia, A.; Scialdone, O. Electrochemical Conversion of CO_2 to HCOOH at Tin Cathode in a Pressurized Undivided Filter-Press Cell. *Electrochim. Acta* **2018**, *277*, 30–40.

(77) Ku, H. Notes on the Use of Propagation of Error Formulas. *J. Res. Natl. Bur. Stand. Sect. C Eng. Instrum.* **1966**, *70C*, 263.

(78) Li, H.; Oloman, C. Development of a Continuous Reactor for the Electro-Reduction of Carbon Dioxide to Formate - Part 1: Process Variables. *J. Appl. Electrochem.* **2006**, *36*, 1105–1115.

(79) Li, H.; Oloman, C. Development of a Continuous Reactor for the Electro-Reduction of Carbon Dioxide to Formate - Part 2: Scale-up. *J. Appl. Electrochem.* **2007**, *37*, 1107–1117.

(80) Zhong, H.; Fujii, K.; Nakano, Y. Effect of $KHCO_3$ Concentration on Electrochemical Reduction of CO_2 on Copper Electrode. *J. Electrochem. Soc.* **2017**, *164*, F923–F927.

(81) Chen, L. D.; Urushihara, M.; Chan, K.; Nørskov, J. K. Electric Field Effects in Electrochemical CO_2 Reduction. *ACS Catal.* **2016**, *6*, 7133–7139.

(82) Singh, M. R.; Goodpaster, J. D.; Weber, A. Z.; Head-Gordon, M.; Bell, A. T. Mechanistic Insights into Electrochemical Reduction of CO_2 over Ag Using Density Functional Theory and Transport Models. *Proc. Natl. Acad. Sci.* **2017**, *114*, E8812–E8821.

(83) Weekes, D. M.; Salvatore, D. A.; Reyes, A.; Huang, A.; Berlinguette, C. P. Electrolytic CO_2 Reduction in a Flow Cell. *Acc. Chem. Res.* **2018**, *51*, 910–918.

(84) Endrodi, B.; Bencsik, G.; Darvas, F.; Jones, R.; Rajeshwar, K.; Janáky, C. Continuous-Flow Electroreduction of Carbon Dioxide. *Prog. Energy Combust. Sci.* **2017**, *62*, 133–154.

(85) Scialdone, O.; Galia, A.; Nero, G. L.; Proietto, F.; Sabatino, S.; Schiavo, B. Electrochemical Reduction of Carbon Dioxide to Formic Acid at a Tin Cathode in Divided and Undivided Cells: Effect of Carbon Dioxide Pressure and Other Operating Parameters. *Electrochim. Acta* **2016**, *199*, 332–341.

(86) Sonin, A. A.; Isaacson, M. S. Optimization of Flow Design in Forced Flow Electrochemical Systems, with Special Application to Electrodialysis. *Ind. Eng. Chem. Process Des. Dev.* **1974**, *13*, 241–248.

(87) Alvarez-Guerra, M.; Del Castillo, A.; Irabien, A. Continuous Electrochemical Reduction of Carbon Dioxide into Formate Using a Tin Cathode: Comparison with Lead Cathode. *Chem. Eng. Res. Des.* **2014**, *92*, 692–701.

(88) Li, H.; Oloman, C. The Electro-Reduction of Carbon Dioxide in a Continuous Reactor. *J. Appl. Electrochem.* **2005**, *35*, 955–965.

(89) McCrory, C. C. L.; Jung, S.; Ferrer, I. M.; Chatman, S. M.; Peters, J. C.; Jaramillo, T. F. Benchmarking Hydrogen Evolving Reaction and Oxygen Evolving Reaction Electrocatalysts for Solar Water Splitting Devices. *J. Am. Chem. Soc.* **2015**, *137*, 4347–4357.

(90) Alabi, A.; AlHajaj, A.; Cseri, L.; Szekely, G.; Budd, P.; Zou, L. Review of Nanomaterials-Assisted Ion Exchange Membranes for Electromembrane Desalination. *npj Clean Water* **2018**, *1*, 10.

(91) Dekel, D. R. Review of Cell Performance in Anion Exchange Membrane Fuel Cells. *J. Power Sources* **2018**, *375*, 158–169.

(92) Hagesteijn, K. F. L.; Jiang, S.; Ladewig, B. P. A Review of the Synthesis and Characterization of Anion Exchange Membranes. *J. Mater. Sci.* **2018**, *53*, 11131–11150.

(93) Jaroszek, H.; Dydo, P. Ion-Exchange Membranes in Chemical Synthesis - A Review. *Open Chem.* **2016**, *14*, 1–19.

(94) Luo, T.; Abdu, S.; Wessling, M. Selectivity of Ion Exchange Membranes: A Review. *J. Memb. Sci.* **2018**, *555*, 429–454.

(95) Maurya, S.; Shin, S.-H.; Kim, Y.; Moon, S.-H. A Review on Recent Developments of Anion Exchange Membranes for Fuel Cells and Redox Flow Batteries. *RSC Adv.* **2015**, *5*, 37206–37230.

(96) Park, C. H.; Lee, S. Y.; Hwang, D. S.; Shin, D. W.; Cho, D. H.; Lee, K. H.; Kim, T.-W.; Kim, T.-W.; Lee, M.; Kim, D.-S.; Doherty, C. M.; Thornton, A. W.; Hill, A. J.; Guiver, M. D.; Lee, Y. M. Nanocrack-Regulated Self-Humidifying Membranes. *Nature* **2016**, *532*, 480–483.

(97) Yee, R.; Rozendal, R.; Zhang, K.; Ladewig, B. Cost Effective Cation Exchange Membranes: A Review. *Chem. Eng. Res. Des.* **2012**, *90*, 950–959.

(98) Trasatti, S.; Petrii, O. Real Surface Area Measurements in Electrochemistry. *J. Electroanal. Chem.* **1992**, *327*, 353–376.

(99) Łukaszewski, M. Electrochemical Methods of Real Surface Area Determination of Noble Metal Electrodes - an Overview. *Int. J. Electrochem. Sci.* **2016**, *11*, 4442–4469.

(100) Del Castillo, A.; Alvarez-Guerra, M.; Solla-Gullón, J.; Sáez, A.; Montiel, V.; Irabien, A. Sn Nanoparticles on Gas Diffusion Electrodes: Synthesis, Characterization and Use for Continuous CO_2 Electroreduction to Formate. *J. CO2 Util.* **2017**, *18*, 222–228.

(101) Yang, H.; Kaczur, J. J.; Sajjad, S. D.; Masel, R. I. Electrochemical Conversion of CO_2 to Formic Acid Utilizing Sustainion Membranes. *J. CO2 Util.* **2017**, *20*, 208–217.

(102) Kaczur, J. J.; Yang, H.; Liu, Z.; Sajjad, S. D.; Masel, R. I. Carbon Dioxide and Water Electrolysis Using New Alkaline Stable Anion Membranes. *Front. Chem.* **2018**, *6*, 1–16.

(103) Proietto, F.; Galia, A.; Scialdone, O. Electrochemical Conversion of CO_2 to HCOOH at Tin Cathode: Development of a Theoretical Model and Comparison with Experimental Results. *ChemElectroChem* **2018**, 1–12.

Table 1: Advantages and disadvantages of bipolar membranes (BPMs) and cation exchange membranes (CEMs) for CO_2 electrolysis.[49,51,90–97]

Membrane	BPM	CEM
Advantages	+ Maintains constant pH + Low product crossover + Low electrolyte contamination + Acidification & basification	+ Low price + Low potential drop + Easy manufacturing + High stability/lifetime
Disadvantages	- High price - Complex manufacturing - Short lifetime - Low stability in strong bases - Delamination of layers - Limits on high ion concentrations	- High product crossover - High electrolyte contamination - Acidic anolyte - pH imbalance

Table 2: Comparison of CO_2 electrolysis to formic acid/formate in continuous flow electrolyzers using Sn-based gas diffusion electrodes and plates.

Conditions	Ref.[100]	Ref.[101]	Ref.[87]	Ref.[76]	This work
Mode of operation	single pass	single pass	single pass	recycled	recycled
Temperature (K)	ambient	ambient	ambient	ambient	ambient
Pressure (Bar)	1	1	1	30	50
Cathode	Sn/C-GDE	Sn/C-GDE	Sn plate	Sn plate	Sn plate
Anode	Ir-MMO	IrO_2	Ir-MMO	Ti/IrO_2-Ta_2O_5	Ir-MMO
Cation exchange membrane	Nafion 117	Nafion 324[a]	Nafion 117	no membrane	Fumasep BPM
Anion exchange membrane	-	Sustainion[a]	-	no membrane	Fumasep BPM
Geometric surface area of cathode (cm^2)	10.0	5	10	9	80
Flowrate/area of cathode ($ml/min{\cdot}cm^2$)	0.07	0.02	2.3	3.3	0.125
Cell voltage (V)	4.3	3.3	2.79	6.5[b]	3.5 (4.0)[c]
Current density (mA/cm^2)	200	140	12.25	50	30 (100)
Concentration of formic acid (% wt)	1.68	9.4	0.005	1.26	1.0 (2.0)
Faraday efficiecy of formic acid (%)	42.3	94	71.4	82.5	90 (65)
Formic acid production rate ($mmol/m^2{\cdot}s$)	4.38	6.8	0.46	2.1	2 (4)
Max. operation time (hrs)	1.5	142	1.5	60	0.33

[a] A three compartment cell with two different types of membranes was used

[b] Cell potential data obtained from Proietto et al.[76] through personal communication

[c] Data in brackets are for a cell potential of 4.0 V

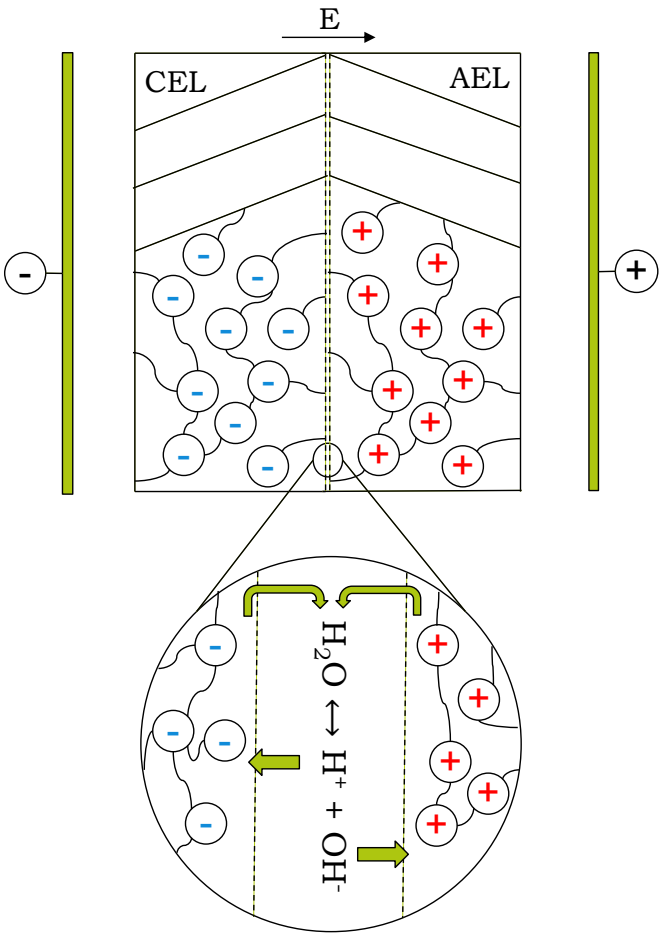

Figure 1: Operating principle of a BPM in reverse bias mode. Applying a sufficiently high potential over the membrane will result in enhanced water dissociation at the AEL-CEL interface, where the protons and hydroxide ions migrate through the CEL and AEL, respectively. The black arrow indicates the direction of the electric field.

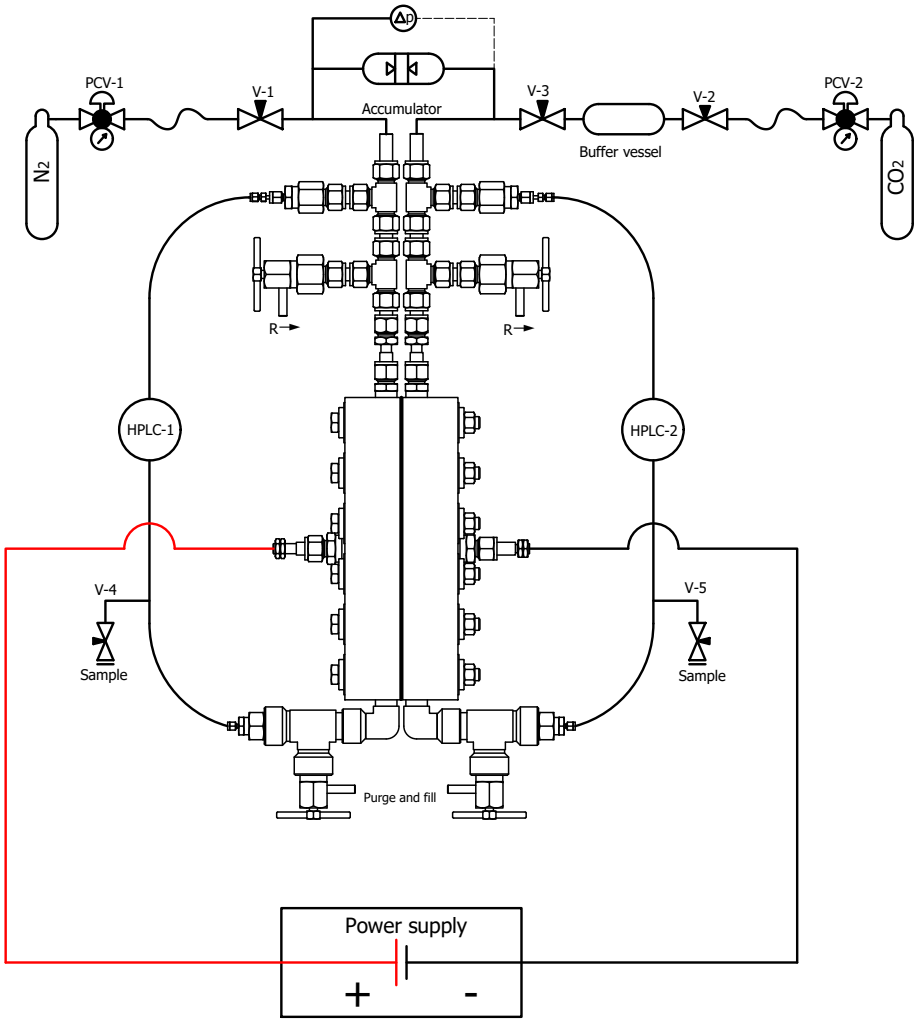

Figure 2: Overview of the high pressure experimental setup. At the core is a high pressure electrochemical reactor, which is divided into two compartments using an ion exchange membrane. The anolyte and catholyte were pressurized by N_2 and/or CO_2 gas cylinders and recirculated with HPLC-pumps. An accumulator was used to eliminate pressure differences between both compartments and to prevent mixing of gaseous reactants and products. The electrochemical experiments were performed at fixed cell potentials using a lab power supply.

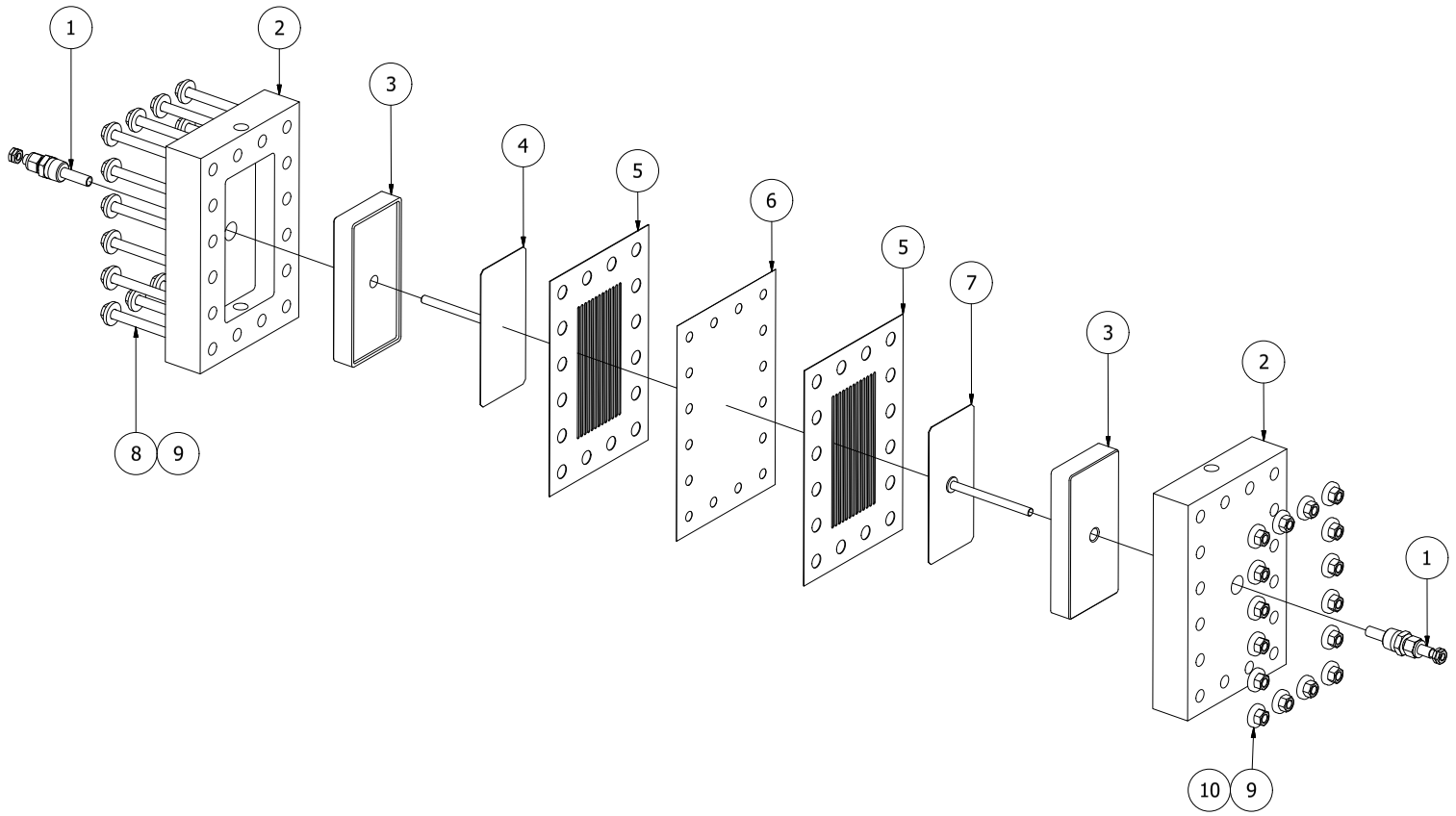

Figure 3: Exploded view of the reactor. (1) Insulator, (2) Reactor shell, (3) Teflon fluid distributor, (4) Anode, (5) Teflon spacer and seal, (6) Membrane, (7) Cathode, (8) Hex head bolt, (9) Isolating washer, (10) Hex nut.

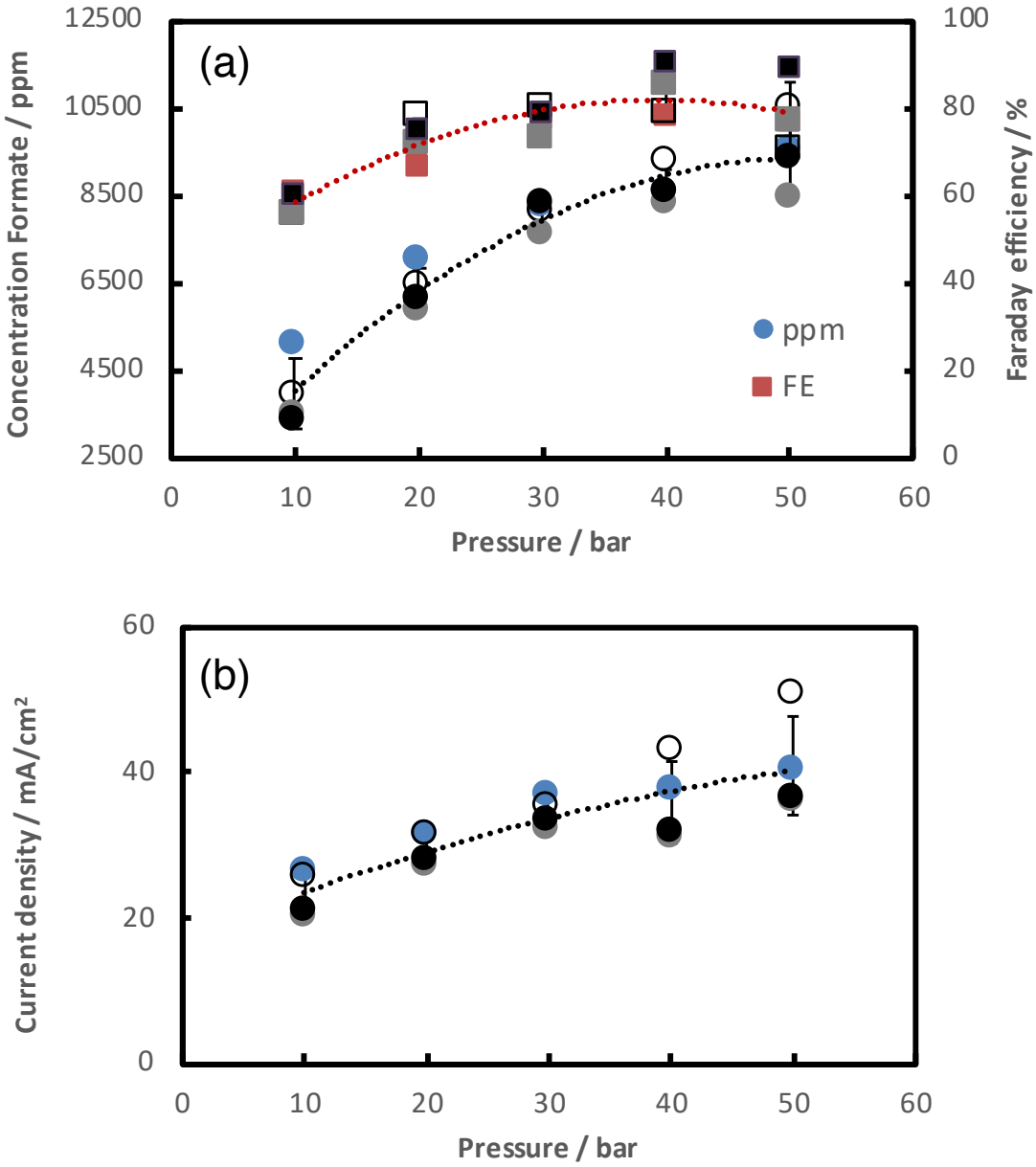

Figure 4: (a) Concentration of formate (circles) and Faraday efficiency (squares), and (b) current density as a function of pressure for CO_2 electrolysis at 3.5 V using a BPM. The anolyte, catholyte, flow rate, and electrolysis time were 1M KOH, 0.5M $KHCO_3$, 10 ml/min, and 20 minutes. Data are shown for four different runs, where the dotted lines represent the arithmetic mean of the results.

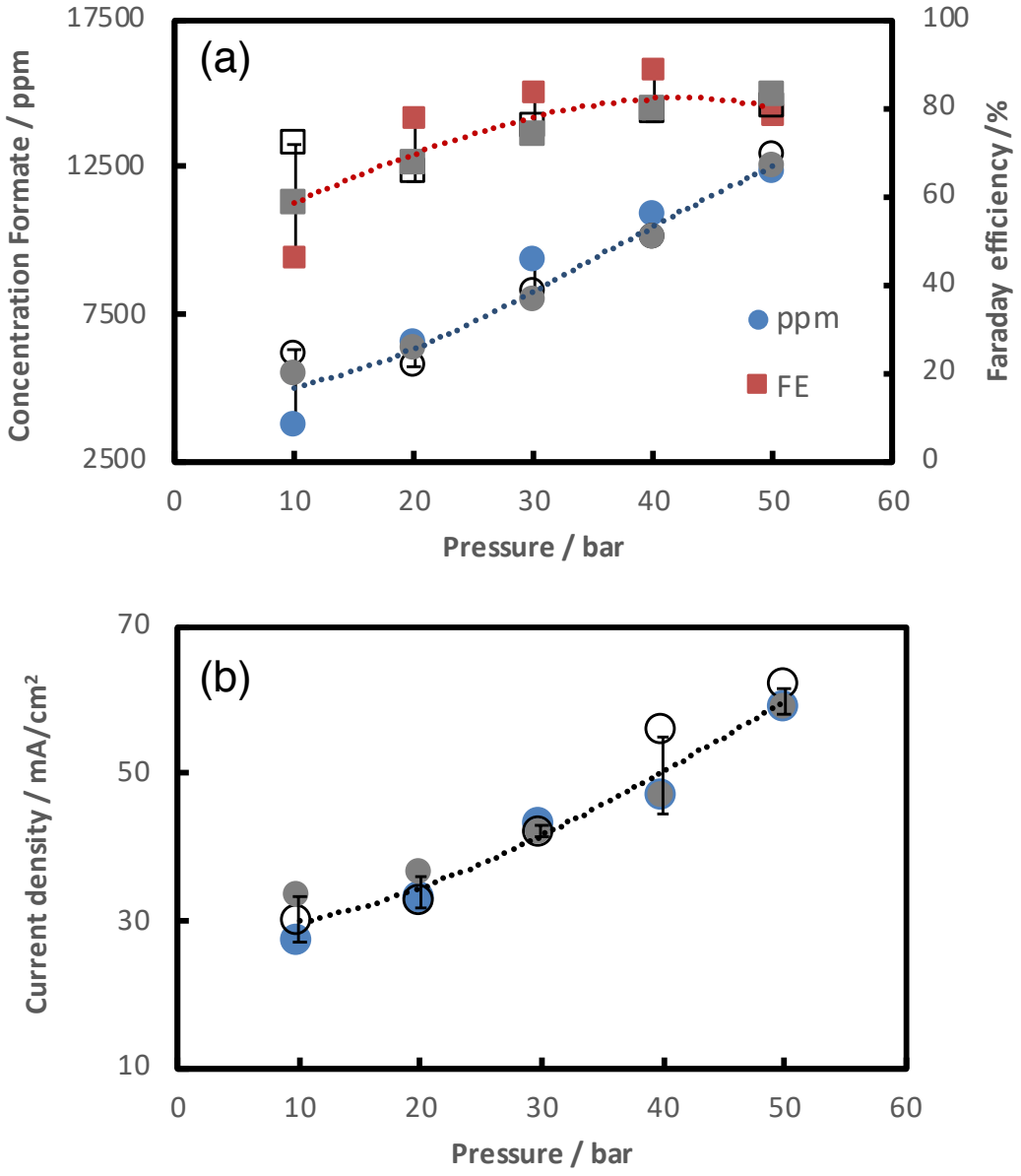

Figure 5: (a) Concentration of formate (circles) and Faraday efficiency (squares), and (b) current density as a function of pressure for CO_2 electrolysis at 3.5 V using a CEM. The anolyte, catholyte, flow rate, and electrolysis time were 0.5M H_2SO_4, 1M $KHCO_3$, 10 ml/min, and 20 minutes. Data are shown for three different runs, where the dotted lines represent the arithmetic mean of the results.

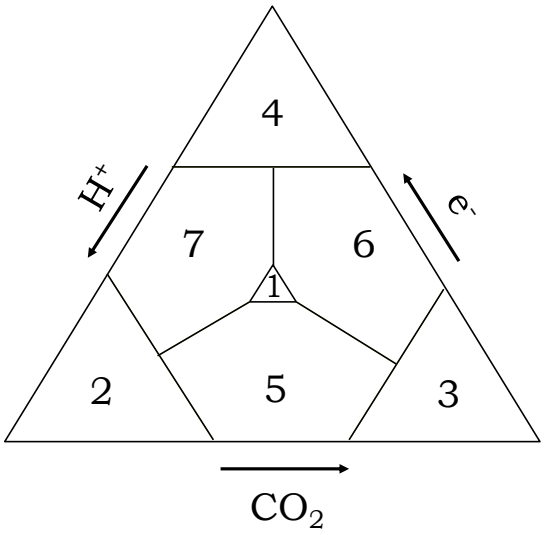

Figure 6: Qualitative triangular schematic diagram to explain the FE for CO_2 electrolysis to formic acid/formate. Region 1 has a correct CO_2, H^+, and e^- stoichiometry, region 2 is deficient in CO_2 and electrons, region 3 is deficient in H^+ and electrons, region 4 is deficient in CO_2 and H^+, region 5 is deficient in electrons, region 6 is deficient in H^+, and region 7 is deficient in CO_2. The axes represent the concentrations of CO_2, electrons and protons on a reaction site of the electrode.

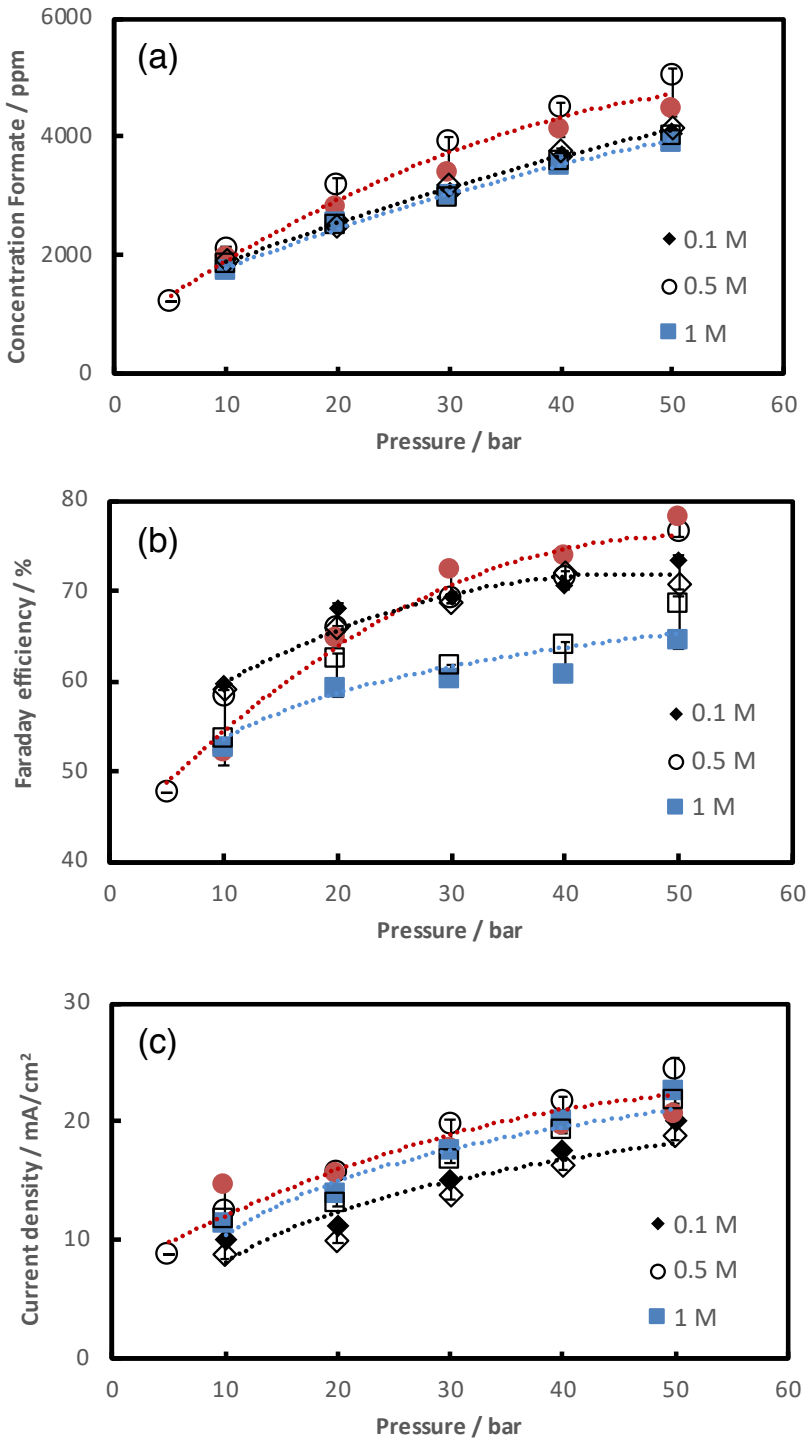

Figure 7: Effect of catholyte concentration on (a) the production of formate, (b) the Faraday efficiency, and (c) the current density as a function of pressure for CO_2 electrolysis at 3 V using a BPM and 0.1M $KHCO_3$ (diamonds), 0.5M $KHCO_3$ (circles), and 1M $KHCO_3$ (squares) as the catholyte. The anolyte, flow rate, and electrolysis time were 1M KOH, 10 ml/min, and 20 minutes. Results are shown for two different runs, where the dotted lines represent the arithmetic mean of the results.

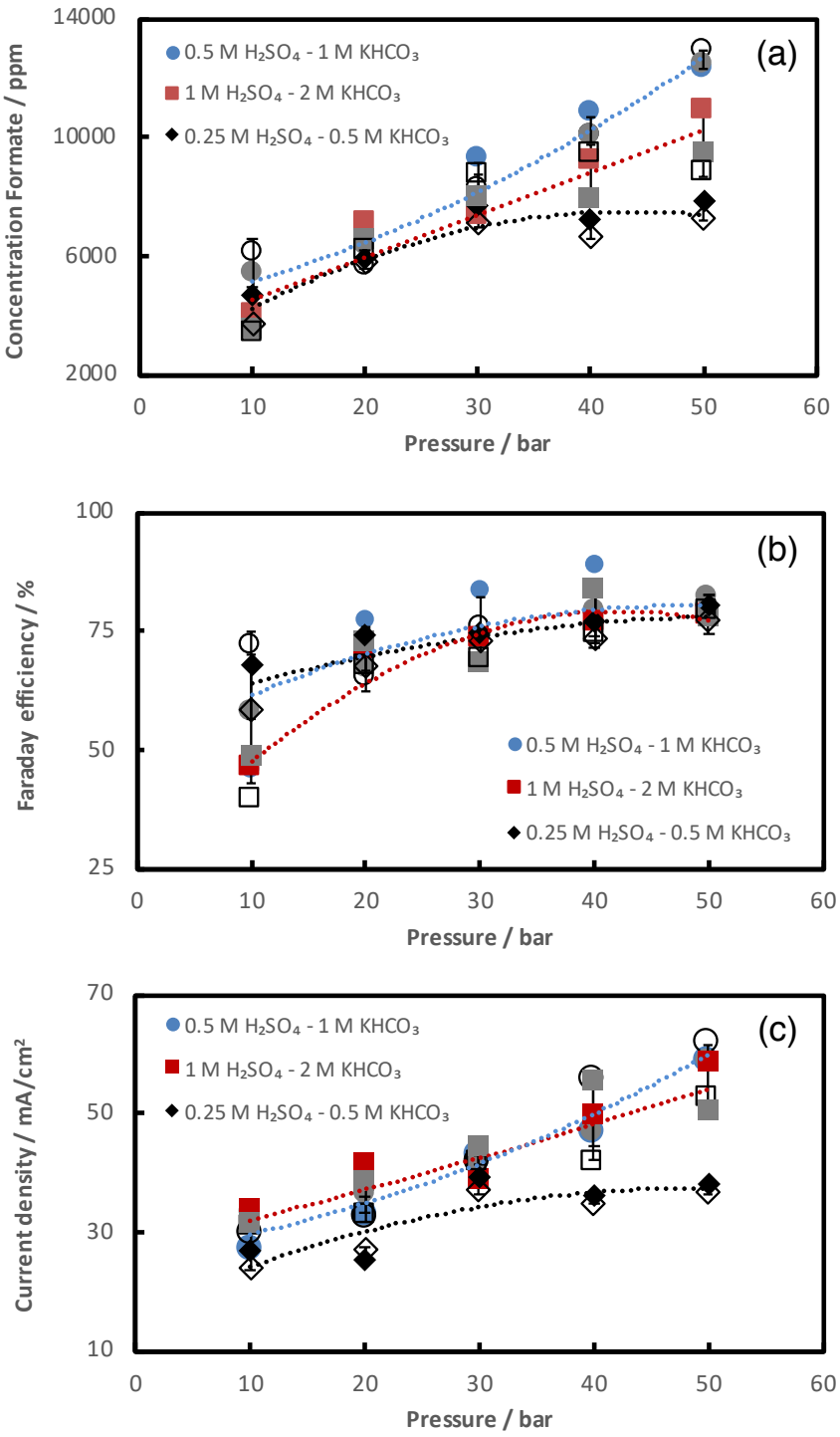

Figure 8: Effect of electrolyte concentration on (a) the formate production, (b) the Faraday efficiency, and (c) the current density as a function of pressure for CO_2 electrolysis at 3.5 V using a CEM. The anolyte, catholyte, flow rate, and electrolysis time were H_2SO_4, $KHCO_3$, 10 ml/min, and 20 minutes. Three different concentrations of anolytes and catholytes were tested; 0.25M H_2SO_4 - 0.5M $KHCO_3$ (diamonds), 0.5M H_2SO_4 - 1M $KHCO_3$ (circles), and 1M H_2SO_4 - 2M $KHCO_3$ (squares). Results are shown for three different runs, where the dotted lines represent the arithmetic mean of the results.

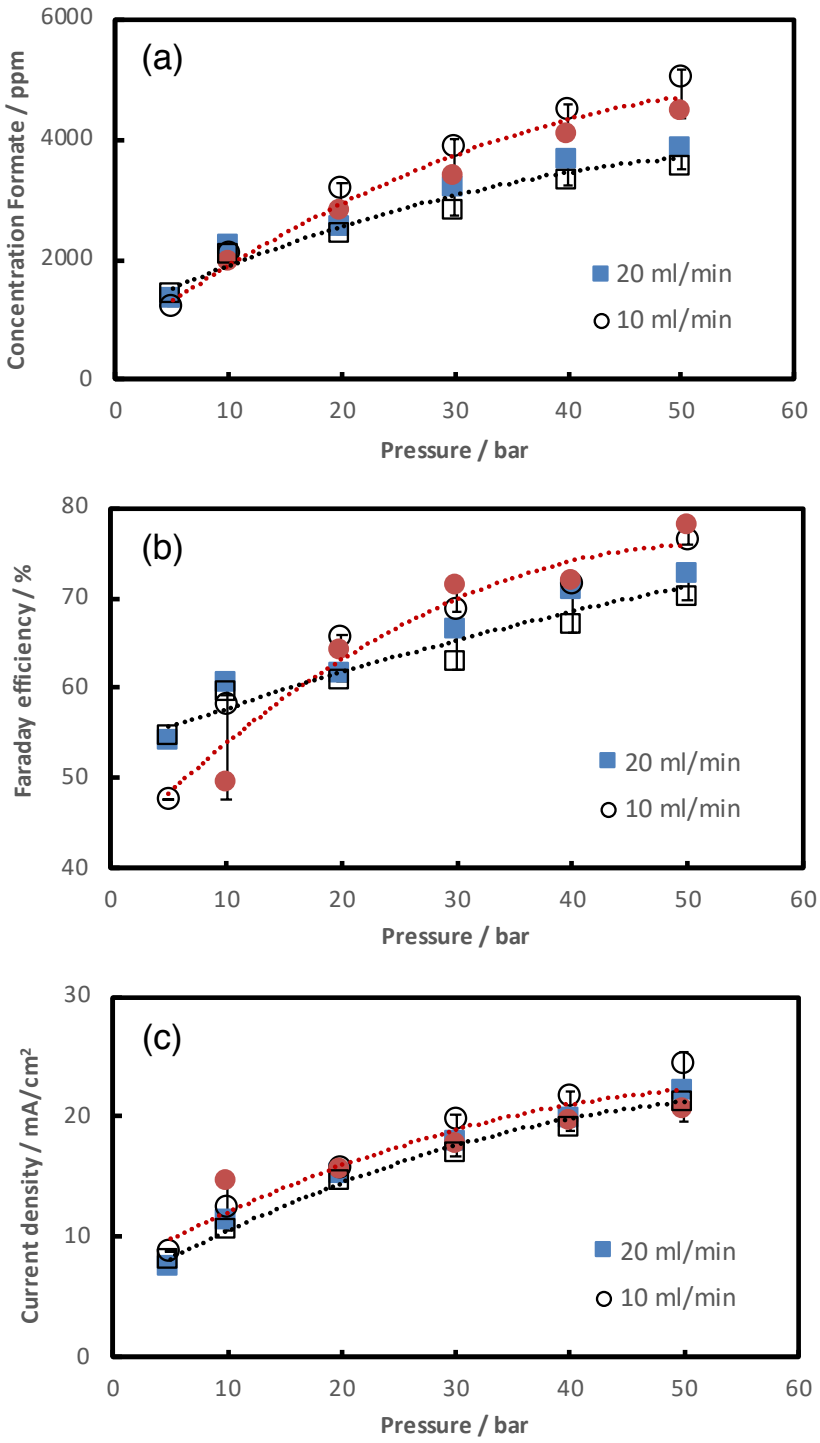

Figure 9: Effect of flow rate on (a) the formate production, (b) the Faraday efficiency, (c) the current density as a function of pressure for CO_2 electrolysis at 3 V using a BPM. The anolyte, catholyte, and electrolysis time were 1M KOH, 0.5M $KHCO_3$, and 20 minutes. Data are shown for two different runs, where the dotted lines represent the arithmetic mean of the results.

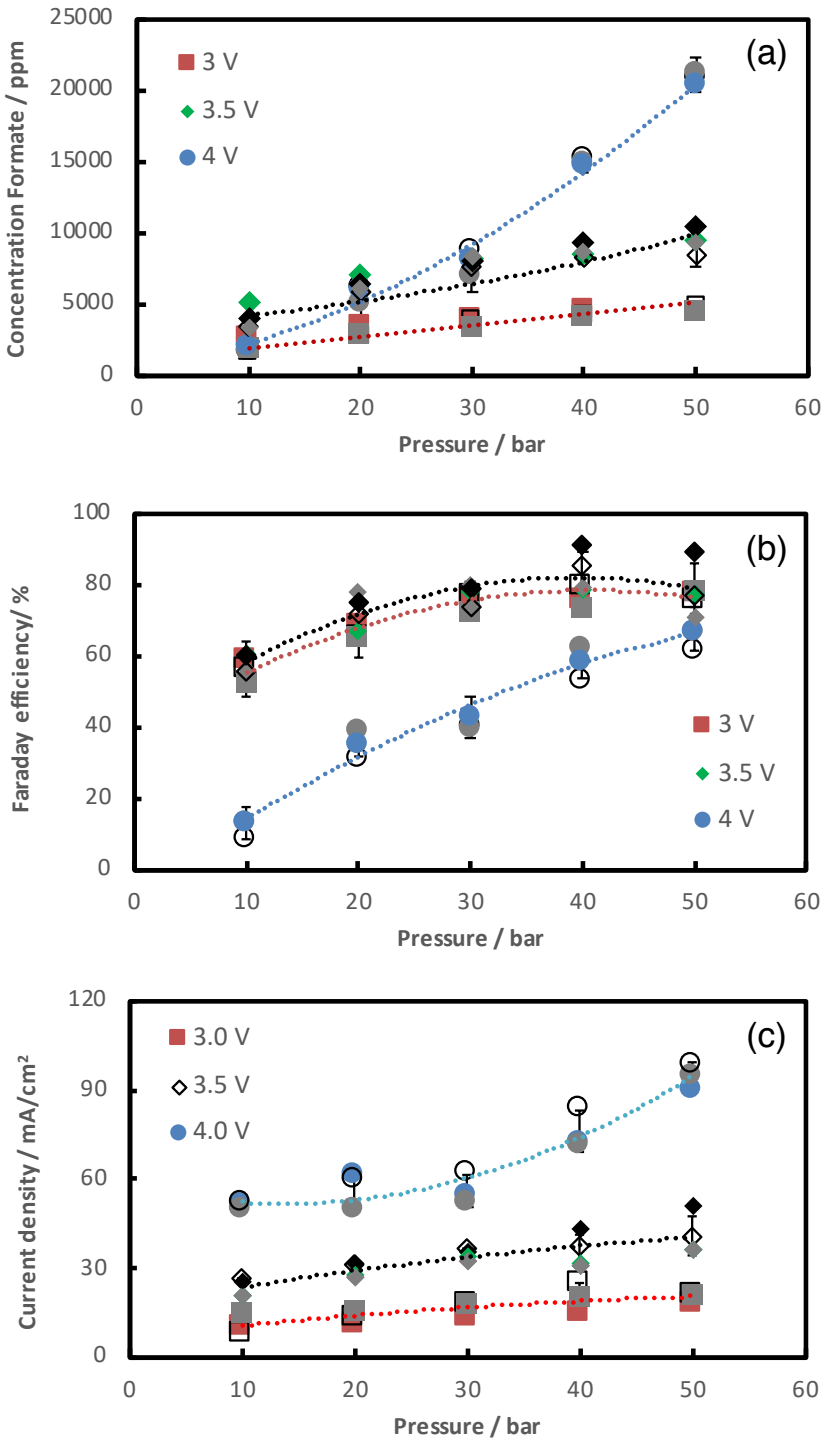

Figure 10: Effect of cell potential on (a) the formate production, (b) the Faraday efficiency, and (c) the current density as a function of pressure for CO_2 electrolysis at 3 V (squares), 3.5 V (diamonds), and 4 V (circles) using a BPM. The anolyte, catholyte, flow rate, and electrolysis time were 1M KOH, 0.5M $KHCO_3$, 10 ml/min, and 20 minutes. Data are shown for three different runs, where the dotted lines represent the arithmetic mean of the results.

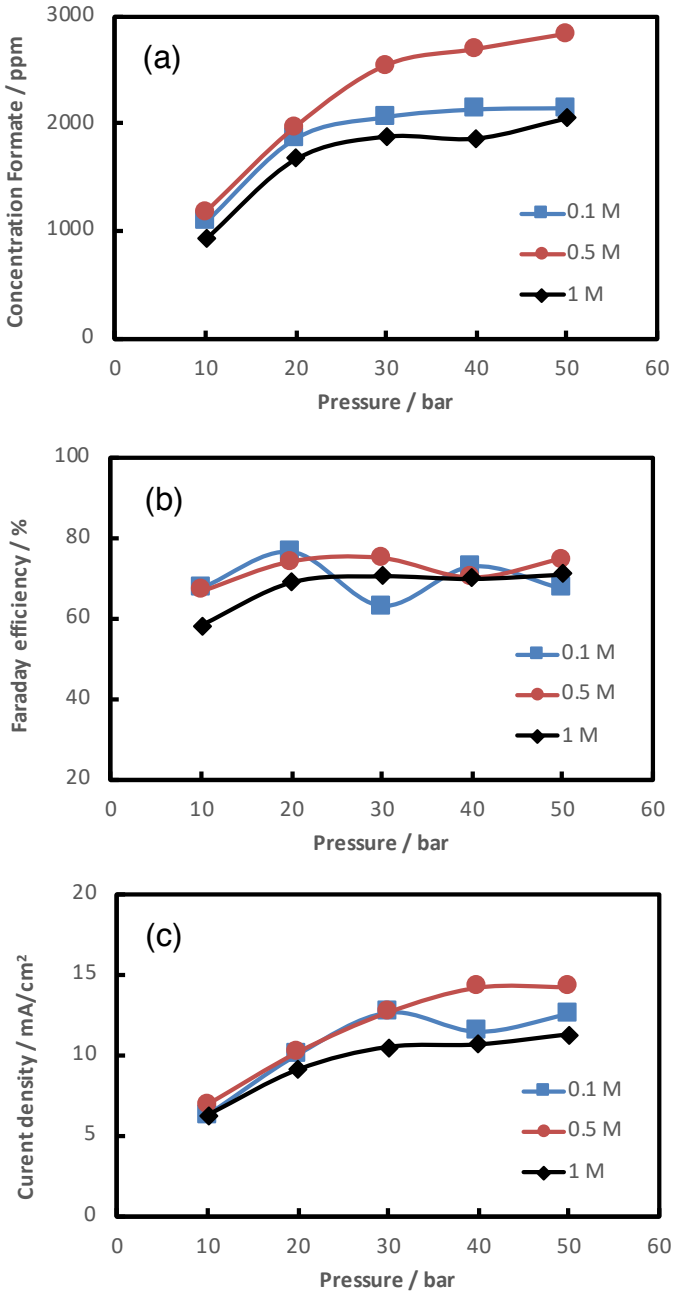

Figure 11: Effect of acidic anolyte on (a) the formate production, (b) the Faraday efficiency, and (c) the current density as a function of pressure for CO_2 electrolysis at 3.5 V using a BPM. The anolyte, flow rate, and electrolysis time were 0.1M H_2SO_4, 10 ml/min, and 20 minutes. Three different concentrations of $KHCO_3$ was used as the catholyte; 0.1M (squares), 0.5M (circles), and 1M (diamonds).

Graphical TOC Entry